

# Group-wise registration of large image dataset by hierarchical clustering and alignment

Qian Wang<sup>a</sup>, Liya Chen<sup>a</sup>, Dinggang Shen<sup>\*b</sup>

<sup>a</sup>Department of Electronic Engineering, Shanghai Jiao Tong University, Shanghai, China

<sup>b</sup>Department of Radiology and BRIC, University of North Carolina at Chapel Hill, NC

## ABSTRACT

Group-wise registration has been proposed recently for consistent registration of all images in the same dataset. Since all images need to be registered simultaneously with lots of deformation parameters to be optimized, the number of images that the current group-wise registration methods can handle is limited due to the capability of CPU and physical memory in a general computer. To overcome this limitation, we present a hierarchical group-wise registration method for feasible registration of large image dataset. Our basic idea is to decompose the large-scale group-wise registration problem into a series of small-scale registration problems, each of which can be easily solved. In particular, we use a novel affinity propagation method to hierarchically cluster a group of images into a pyramid of classes. Then, images in the same class are group-wisely registered to their own center image. The center images of different classes are further group-wisely registered from the lower level to the upper level of the pyramid. A final atlas for the whole image dataset is thus synthesized when the registration process reaches the top of the pyramid. By applying this *hierarchical image clustering* and *atlas synthesis* strategy, we can efficiently and effectively perform group-wise registration to a large image dataset and map each image into the atlas space. More importantly, experimental results on both real and simulated data also confirm that the proposed method can achieve more robust and accurate registration than the conventional group-wise registration algorithms.

**Keywords:** Group-wise registration, hierarchical registration, image clustering

## 1. INTRODUCTION

Medical image registration has attracted a lot of scientific interest during the past decades. It is highly needed in clinical researches and applications for integration and comparison of data from different subjects or groups, and for construction of statistical atlas to reflect structural and functional variability within a population. Most reported registration methods were developed for pair-wise registration, i.e., registering a selected template to an individual image for spatial normalization or atlas-based segmentation. Although the template can be selected in different ways according to the specific problems under study, the subjective selection of the template can eventually introduce unavoidable bias to the subsequent analysis of image data. Further, with advances of imaging and storage technologies, more imaging data are acquired for research, which call for more effective methods to register large sets of images.

To deal with these problems, group-wise registration was proposed recently to simultaneously register a group (instead of a pair) of images. By simultaneous registration of all individual images, the group-wise registration methods are able to achieve consistent registration across all images and establish anatomical correspondences within all images in the group [1][2]. On the other hand, the atlas produced by group-wise registration can better represent a specific group, and the performance of subsequent comparison and analysis upon the groups of image data can also be improved. Several group-wise registration methods have been proposed in the literature. In [3], the atlas was produced by averaging deformation fields generated from all possible pair-wise registrations. In [4], the atlas was determined as the closest image to the actual template by applying multi-dimensional scaling to all pair-wise registrations. These methods (as in [3][4]) achieve group-wise registration by taking advantage of pair-wise registrations, but they suffer from the accompanying high computational complexity when the number of images to be registered increases and more pair-wise registrations need to be performed.

---

\* Email: dgshen@med.unc.edu; Tel: 919-966-3535.

Accordingly, several methods have been developed for faster and more robust group-wise registration. In [5], the final atlas was constructed within a diffeomorphic framework, which had been successfully applied to pair-wise registration before. Also, a congealing framework based group-wise registration method was proposed in [6]. With an information-theoretic objective function and a gradient-based stochastic optimizer, each image in the group can approach their center image simultaneously. Also, an unbiased atlas can be generated as a by-product when registration completes. This group-wise registration framework [6] was inherited and extended later by Balci *et al* [7] as a non-rigid group-wise registration method, by introducing free-form B-splines to represent image transformations. However, in order to group-wisely register all images simultaneously, Balci's method [7] can handle only a small group of images (e.g., dozens) due to the limitation of hardware in a general computer. Also, the speed and the robustness of this algorithm might become a problem when a large image dataset needs to be registered simultaneously. To overcome these limitations, we present a novel hierarchical group-wise registration framework as detailed below.

## 2. METHOD

A hierarchical group-wise registration framework is designed in the following to decompose a *large-scale* group-wise registration problem into a series of *small-scale* group-wise registration problems. The small-scale problems are independently solved one by one, and their produced results are then hierarchically synthesized following a “*down-to-up*” fashion to construct the final atlas for a large image dataset, which might include hundreds or even thousands of images.

### 2.1 Hierarchical image clustering

As we have mentioned, all images in the whole group are clustered into several different classes, with each class only containing the spatially-close images. For image clustering, a common approach as in the classical *k*-means method is to determine a subset of exemplars from all images, so that the sum of distances between exemplars and other images could be minimized. Usually, the determination of exemplars in the very beginning of image clustering is just a random selection, which could greatly deteriorate the robustness of the clustering results. Furthermore, the number of classes in the *k*-means method has to be manually set before clustering, which implies that the arbitrarily determined number of classes may not accurately reflect the intrinsic distribution of images in their high-dimensional space.

A novel clustering method, namely affinity propagation (AP) [8], is employed in our registration framework for image clustering. Different from classical clustering methods, the affinity propagation method connects each image to a specific node in a network, and considers all images as potential exemplars of different classes without any arbitrary priorities. To cluster images from a dataset via the affinity propagation method, the real-valued similarity measure between each pair of images should be input. Various definitions of image similarity measures could be used here. A simple example is the least square error (LSE) of intensities of all images under consideration.

In this paper, we have adopted mutual information (MI) [9] as a selected similarity measure for the affinity propagation method, although other similarity measures such as normalized mutual information (NMI) [10] can also be applied. In particular, when the overlapping volume of two images is relatively tiny, normalized mutual information could better reflect the geometrical distance between the two images than mutual information [10]. However, considering the fact that all images in our following experiments have been linearly aligned before image clustering performed, it is sufficient for mutual information to measure the similarity of images.

Besides the measurement of similarity between each pair of images, self-similarity should also be pre-defined before the affinity propagation method is used to cluster images. The value of self-similarity indicates the possibility for a certain image to be exemplar in a detected class. As a result, different images should be assigned with the same self-similarity, thus allowing them to compete equally for exemplars and form their individual classes. Meanwhile, self-similarity could distribute within the range between the minimum of pair-wise similarity measures (which can lead to fewer detected classes) and the median of all measures (which can result in more detected classes) [8]. Since our goal here is to decompose the large-scale group-wise registration problem into a series of small-scale registration problems, it is better to have a reasonable number of classes, each of which includes similar number of images. In this way, we select the median of input pair-wise similarity measures as self-similarity.

After clustering, we can obtain a certain number of detected classes. However, some classes might be of relatively large sizes, which are beyond the number that the current group-wise registration algorithms can successfully handle. To solve

this problem, the affinity propagation clustering method is iterated within each of those large classes until the sizes of all children classes are under a certain threshold, which guarantees that each small class could be group-wisely registered via the contemporary group-wise registration methods. By following this strategy, we can finally establish a pyramid as shown in Fig. 1, which contains classes of images at different levels. In Fig. 1, each node indicates a corresponding class and the top node represents the whole large image dataset. In the pyramid, similar images can be contained within the same class/node, while non-similar images might be placed in different classes/nodes that could be apart greatly from each other.

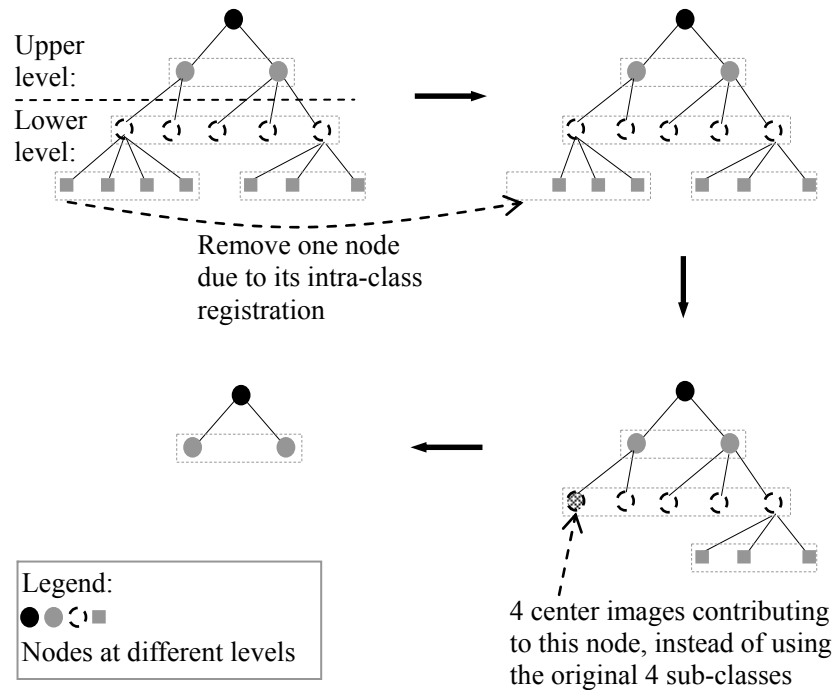


Fig. 1. A pyramid of hierarchical classes of images. Each node in the pyramid denotes a class with a small number of images after clustering. The link between two nodes at different levels indicates that the node at the lower level contains a sub-class of images belonging to the class represented by the node at the upper level. Also, the down-to-up atlas synthesis is demonstrated by solid arrows in this figure.

## 2.2 Atlas synthesis

Based on the image pyramid produced through hierarchical image clustering, we can gradually perform group-wise registration “down-to-up”, and finally construct the atlas for the whole image dataset. Different from the previous “up-to-down” image clustering stage, this hierarchical registration stage starts from the lowermost level of the pyramid and ends at the uppermost level. All images in a specific class (or a node of the pyramid) are group-wisely registered to produce their own center image. All center images of different classes (or different nodes of the pyramid) will then be incorporated and group-wisely registered in their same parent node (at a higher level). By repeating these steps, we can eventually “destroy” the pyramid, construct the atlas for the large image dataset, and register all input images to the constructed atlas.

Specifically, for each node which only contains member images except for children nodes, the intra-class group-wise registration is performed independently in the very beginning. Since the number of images within each node/class has been controlled during the hierarchical image clustering stage, the group-wise registration of images in each node could be well handled, i.e., using Balci’s group-wise registration algorithm [7] freely available in ITK. After the intra-class registration for a certain node, the corresponding center image is constructed to represent the respective class. Then, the node denoting that already registered class is removed from the pyramid, while the center image of the respective class is

added as a new member image into its parent node (c.f. Fig. 1). By repeating those intra-class registration and node removal steps, the internal levels of the pyramid can be gradually reduced, and the group-wise registration of a large image dataset is decomposed to a hierarchical series of group-wise registrations of small numbers of images (including center images from classes at lower levels). Thus, the final atlas for the whole image dataset can be hierarchically constructed, and all images could be registered to the constructed atlas. The process of this atlas synthesis stage is demonstrated in Fig. 1.

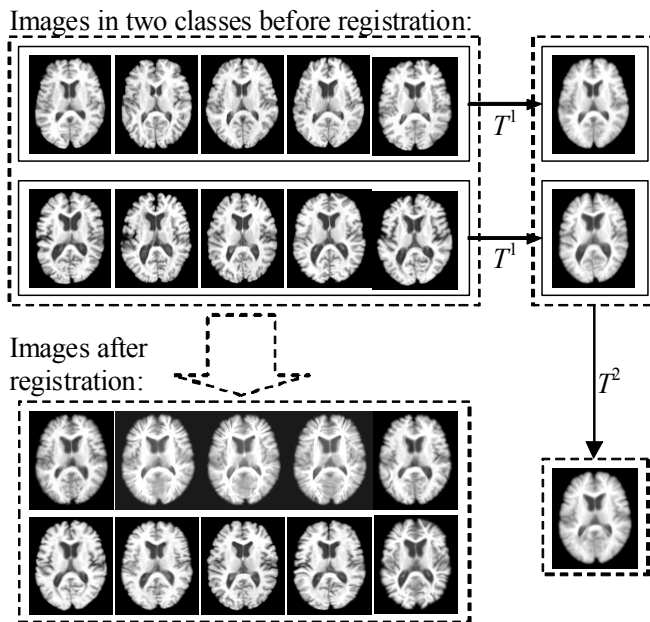


Fig. 2. Demonstration of the atlas synthesis stage. 10 images are clustered into 2 classes, and the registration is decomposed into two steps indicated by solid arrows. The registration results for images in each class are respectively shown in the bottom. The final atlas for all 10 images is constructed in the bottom right.

In applications, the input images are contained by leaf nodes in the pyramid. But the leaf nodes themselves are not necessarily at the lowermost level of the pyramid. After the hierarchical registration climbs up the top of the pyramid, each image is combined with a deformation route which connects it to the finally constructed atlas. This deformation route is usually composed of several paths, which connect the original image to the center image of its respective class, to the center images at higher levels, and to the final atlas. Each deformation path represents a particular deformation field estimated during different intra-class registration steps. By concatenating the deformation fields of different paths within a route, a single but complete transformation can be estimated for each image, which can deform each image to the space defined by the constructed atlas. Meanwhile, the inverse of each deformation field is originated from the same space, which can map the constructed atlas to the space of each individual image and help measure various structure sizes in the individual images.

In order to better illustrate the steps of atlas synthesis, we have provided a simple example in Fig. 2. Two classes were detected from 10 images, and each class contains 5 images as shown in the figure. Images in the two classes are group-wisely registered independently, to approach their respective center images through their individually estimated transformations  $\{T_{j,i}^1 | j=1,2; i=1,\dots,5\}$ , where  $j$  denotes a certain class,  $i$  represents an image in the class, and  $T^1$  denotes the transformation at the bottom level of the pyramid. The two centers are further group-wisely registered, leading to the final atlas through the transformations  $\{T_j^2 | j=1,2\}$ . By applying the respective overall transformation which could be written as  $T_j^2(T_{j,i}^1(x_{j,i}))$ , each image  $\{x_{j,i}\}$  can be mapped from its original space into the atlas space, as demonstrated in Fig. 2.

### 3. EXPERIMENTAL RESULTS

In the following, we will use several experiments to demonstrate the performance of our proposed hierarchical group-wise registration framework, and further compare its performance with other methods. We will show that our method is able to perform group-wise registration of a large image dataset with a general computer. We will also show that the introduction of additional image clustering stage for constructing a pyramid of image classes from a large dataset will not necessarily result in more computational time in our method. On the contrary, the overall cost of registration time via our method is significantly saved. Finally, we will demonstrate the ability of our method in capturing morphological changes in brain images, as well as tiny atrophy in the diseased brains.

#### 3.1 Feasibility of group-wise registration of large image dataset

We have employed an image dataset of 159 linearly-aligned brain MR images to demonstrate the feasibility of our hierarchical registration method in group-wise registration of a large image dataset. First, these 159 images are hierarchically clustered and placed into a pyramid of classes as shown in Fig. 3. For convenience, not all images are displayed in the figure; some nodes as well as their children nodes/classes are omitted. However, the general structure of the pyramid is well preserved, i.e., there are 3 levels in this pyramid, and the number of images within any node is constrained to be no more than 20.

Once the pyramid has been constructed through the stage of hierarchical image clustering, the intra-class registration starts to perform from the lowermost level (labeled as ① in Fig. 3) to the uppermost level (labeled as ③ Fig. 3). As the series of registrations continues, different nodes that contain different classes of images gradually merge into one node where the center images of these nodes could be observed as blur images in Fig. 3. Finally, the atlas (label ③) for the whole large image dataset is produced through a relatively simple group-wise registration of 5 images labeled as ② in the pyramid of Fig. 3.

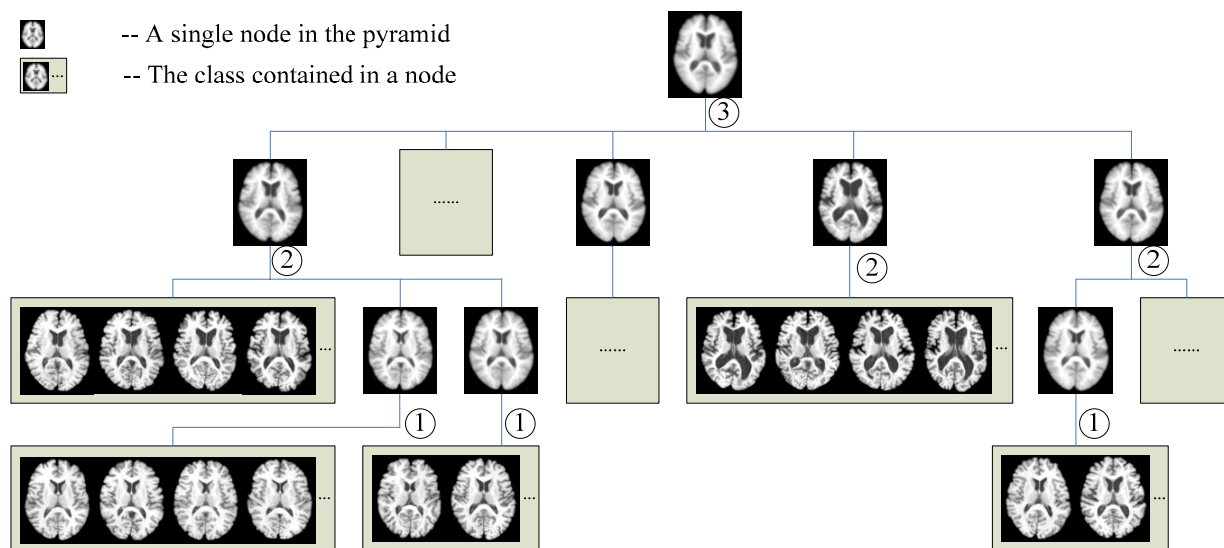


Fig. 3. 150 linearly-aligned brain images are hierarchically clustered into a 3-level pyramid. The intra-class group-wise registration is performed from the lowermost level of the pyramid to the uppermost level, with labels increasing from ① to ③. Note that only some typical images are shown in this figure. The blur images inside are the center images of the respective classes, or the final atlas (labeled as ③).

It spent 8 hours and 40 minutes (including both hierarchical image clustering stage and atlas synthesis stage) to perform our proposed hierarchical group-wise registration on these 159 brain images. Each of these images contains  $83 \times 98 \times 75$

voxels, and the group-wise registration is executed under a single-level registration strategy where 16 B-spline control points are deployed along each axis. The computer used here is powered with an Intel T7250 CPU and 1G RAM. However, using our computer, we found that it is just impossible to simultaneously register all 159 images via Balci's method [7]. There are two reasons: *first*, the memory is a problem to allocate spaces for 159 images and a huge number of B-spline coefficients; *second*, the optimization of this huge number of deformation parameters needs extremely strong computation power and may exceed the capability of a general computer.

### 3.2 Speed performance

We have randomly selected 30 images from the dataset employed above and perform group-wise registration upon the subset of images, in order that the time costs of group-wise registration via both our method and Balci's method [7] could be directly and quantitatively compared. In Table 1, we have provided the detailed time costs of the two methods. Compared to Balci's method, the stage of image clustering in our method causes additional processing time. However, even added with this additional cost, the overall time cost of our method is still much lower than Balci's method which needs 40.4% more. Meanwhile, the quality of group-wise registration does not fall in our method. Specifically, the value of stack entropy, which is defined to measure the closeness of all images in a dataset after registration [11], indicates that both methods have achieved similar registration performances, while our method has slightly smaller stack entropy which implies better registration quality. The reason is that, in our method, all images in the same class (after hierarchical clustering) are spatially close, thus they are relatively easy to be registered to their center. However, in Balci's method, each image has to travel independently to the common center or the final atlas, even though some of them are spatially so close that they could be deformed together to the atlas in order to save processing time and improve the robustness.

Table 1. Comparison of computation time via different methods.

|               |                    | Our method | Balci's method |
|---------------|--------------------|------------|----------------|
| Time<br>Cost  | Clustering Stage   | 4.5 min    | —              |
|               | Registration Stage | 76 min     | 113 min        |
|               | Overall            | 80.5 min   | 113 min        |
| Stack entropy |                    | 0.9903     | 1.0280         |

### 3.3 Ability to capture local morphological features

Deformation fields produced in registration are often used to quantitatively characterize normal and pathologic anatomies [12]. Thus, the estimated deformation fields can be used to evaluate the performance of the group-wise registration method. We used two sets of images, i.e., one includes 12 original images and the other includes 12 images with simulated atrophies in the precentral gyrus (PCG) and the superior temporal gyrus (STG) on each of the 12 original images [13][14]. Fig. 4 shows an example of the original image and its corresponding image with simulated atrophies. The amount of simulated atrophies is around 10% in both PCG and STG.

These 24 images are registered, respectively, via our hierarchical group-wise registration framework and Balci's method [7] under the same constraint of registration. The deformation field connecting each image to the final atlas is estimated after group-wise registration completes. Here, we employ the SPM software [15] to examine the group differences of the Jacobian maps of the inverse deformation fields from the 12 original images to the 12 simulated images. Larger *t*-score in the paired *t*-test achieved within the neighborhood of the simulated atrophy locations indicates that morphological differences between two sets of images are more salient in deformation fields, and implies better registration quality. From Table 2, we could observe that, with the same smoothing kernel size in SPM's paired *t*-test, our method could better detect the simulated atrophies with higher statistical power, reflected as higher *t*-scores obtained for atrophies in both PCG and STG. In another word, our method could better register images to the atlas group-wisely, and enables more accurate detection of simulated atrophies.

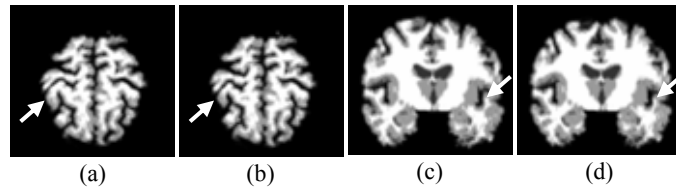


Fig. 4. Example of original MR images and their respective simulated images: (a) and (c) original images; (b) image with simulated atrophy in the precentral gyrus (PCG); (d) image with simulated atrophy in the superior temporal gyrus (STG).

Table 2. Paired t-test results: t-scores at detected atrophies.

|                | Balci's method | Our method |
|----------------|----------------|------------|
| Atrophy in PCG | 14.09          | 18.10      |
| Atrophy in STG | 16.99          | 21.61      |

## 4. CONCLUSION

A novel hierarchical group-wise registration framework has been proposed in this paper. This method integrates the *hierarchical image clustering* as well as the *atlas synthesis* into a single registration framework. Since the group-wise registration of large image dataset has been decomposed into a series of small-scale group-wise registration problems, our method provides a feasible, robust, and accurate way to handle large image datasets. It is challenging for the conventional group-wise registration methods to register a large number of images simultaneously with a general computer, due to the limitation of hardware, especially CPU and memory capabilities. On the other hand, the experimental results in our paper have demonstrated that our method can efficiently and effectively overcome the limitation with respect to the size of image dataset for group-wise registration. Meanwhile, the processing speed of our hierarchical group-wise registration method has been improved with even better registration quality. In the future, we will apply our method to various large clinical studies, to demonstrate its unique performance in clinical applications.

**Acknowledgement:** The author would like to thank Mr. S. K. Balci for his kind help, particularly for our questions in using his group-wise registration algorithm available in ITK. This work is supported partly by grants 1R01EB006733, 1R03EB008760, and 7R03MH076970.

## REFERENCES

- [1] Zitová, B. and Flusser, J., "Image registration methods: a survey," *Image and Vision Computing*, vol. 21, pp. 977-1000 (2003).
- [2] Crum, W.R., Hartkens, T. and Hill, D.L.G., "Non-rigid image registration: theory and practice," *The British Journal of Radiology*, 77, S140-S153 (2004).
- [3] Seghers, D., D'Agostino, E., Maes, F., Vandermeulen D. and Suetens, P., "Construction of a brain template from MR images using state-of-the-art registration and segmentation techniques," *MICCAI 2004, LNCS*, vol. 3216, pp. 696-703 (2004).
- [4] Park, H., Bland, P.H., Hero, A.O. and Meyer, C.R., "Least biased target selection in probabilistic atlas construction," *MICCAI 2005, LNCS*, vol. 3750, pp. 419-426, 2005.

- [5] Joshi, S., Davis, B., Jomier, M. and Gerig, G., "Unbiased diffeomorphic atlas construction for computational anatomy," *NeruoImage*, 23, S151-S160 (2004).
- [6] Zöllei, L., Learned-Miller, E., Grimson, E. and Wells, W.M., "Efficient population registration of 3D data," *CVBIA 2005, LNCS*, vol. 3765, pp. 291-301 (2005).
- [7] Balci, S.K., Golland, P. and Wells, W.M., "Non-rigid group-wise registration using B-spline deformation model," *Workshop on Open-Source and Open-Data for 10-th MICCAI*, pp. 105-121 (2007).
- [8] Frey, B.J. and Dueck, D., "Clustering by passing messages between data points," *Science*, vol. 315, pp. 972-976 (2007).
- [9] Pluim, J.P.W., Maintz, J.B.A. and Viergever, M.A., "Mutual information based registration of medical images: a survey," *IEEE Trans. Medical Imaging*, vol. 22, no. 8, pp. 986-1004 (2003).
- [10] Studholme, C., Hill, D.L.G. and Hawkes, D.J., "An overlap invariant entropy measure of 3D medical image alignment," *Pattern Recognition*, vol. 32, no. 1, pp. 71-86 (1999).
- [11] Miller, E.G., Matsakis, N.E. and Viola, P.A., "Learning from one example through shared densities on transforms," *CVPR 2000*, vol. 1, pp. 464-471 (2000).
- [12] Shen, D. and Davatzikos, C., "HAMMER: hierarchical attribute matching mechanism for elastic registration," *IEEE Trans. Medical Imaging*, vol. 21, pp. 1421-1439 (2002).
- [13] Xue, Z., Shen, D. and Davatzikos, C., "Statistical representation of high-dimensional deformation fields with application to statistically constrained 3D warping," *Medical Image Analysis*, 10:740-751 (2006).
- [14] Davatzikos, C., Genc, A., Xu, D. and Resnick, S.M., "Voxel-based morphometry using the RAVENS maps: methods and validation using simulated longitudinal atrophy," *NeuroImage*, 14, S1361-1369 (2001).
- [15] SPM – Statistical Parametric Mapping, <http://www.fil.ion.ucl.ac.uk/spm/>.